Parametric investigation of substrate temperatures on the properties of Zinc oxide deposited over a flexible polymeric substrate via spray technique

P Rajagopalan[1], Rohit Gagrani[2], Daisuke Nakamura[3], Tatsuo Okada[3], Vipul Singh[4] and I A Palani[1,2]

[1] Centre for Material Science and Engineering, IIT Indore, Indore, India.

[2] Mechatronics and Instrumentation Lab, Department of Mechanical Engineering, IIT Indore, Indore, India.

[3] Department of Electrical and Electronic Systems Engineering, Kyushu University, Kyushu, Japan

[4] Molecular and Nano-electronics Research Group (MNRG), Department of Electrical Engineering, IIT Indore, Indore, India.

Email: palaniia@iiti.ac.in, phd1401181006@iiti.ac.in

Abstract. Here we report the influence of substrate temperature (300-500 °C) on the deposition and growth of ZnO over a Flexible polyimide film. Owing to its simplicity, large area deposition capability and Cost effectivity Spray Pyrolysis technique was used. We have modified the conventional process of Spray pyrolysis by spraying for shorter durations and repeating the process which in turn reduced the Island formation of ZnO. Moreover, this technique helped in maintaining the constant temperature and uniformity during the deposition as prolonged spraying reduces the temperature of the heating plate drastically. Photoluminescence (PL) reveals that at 350 and 400° C the defect have reduced. XRD reveals the crystallinity and Impurities present. FE-SEM reveals the structure morphology changes with the change in the substrate temperature. TGA was done to ensure that substrate does not undergoes dissociation at high temperature. It was observed at the film deposited at 400 ºC was found to be more uniform, defect free and crystalline. Hence, IV characterization of the film deposited at 400 ºC was done which showed good rectification behaviour of the Schottky diodes.

KEYWORDS: semiconductors; thin film; chemical synthesis, flexible substrate.

1. Introduction

ZnO, a wide bandgap semiconductor, has appealed lots of attention of scientists due to its excellent chemical and physical properties, ample morphology and numerous applications in areas of microelectronic and opto-electronic devices viz. LEDs, solar cells, energy harvesting etc.[1-7]. The research in electronics and semiconductor industry is evolving the portability of devices are on the rise. The need for flexible devices are quite visible in the Recent Development [3-7]. Spray pyrolysis

is one such technique which provides large area deposition at a relatively low cost in very less time to meet the current production demands. Here, an attempt is made to deposit Zinc Oxide on the flexible Polymeric Substrate (Polyimide) using Spray Pyrolysis.

An Investigation was carried out to identify the effect of substrate temperature on the growth of ZnO nano structures. The conventional process of Spray pyrolysis was modified by spraying for shorter durations and repeating the process which in turn reduced the Island formation of ZnO. Moreover, this technique helped in maintain the constant temperature and uniformity during the Deposition. As prolonged spraying reduces the temperature of the heating plate drastically. To the best of our knowledge the deposition of ZnO on Polyimide (PI) using spray pyrolysis has yet not been reported. In addition, the structural, optical, thermal and electrical properties of these films have also been studied.

2. Experimental Setup

Anhydrous Zinc Acetate (sigma Aldrich) was used to prepare 0.1 M solution using Methanol (sigma Aldrich) and Deionized water (3:1). Glycol Acetic Acid (Renkem) was added to increase the pH of the solution. The pH was maintained around 3.5 to 4. The solution was stirred at relatively High rpm on a magnetic stirrer at room temperature. It was kept for some time so that the undissolved particles may settle down. This was again followed by stirring at high RPM for 48 hours. The beaker were tightly covered with aluminum foil.

Later, the 50ml solution holder was utilized for the spraying. Fresh Nylon tubes thoroughly cleaned with Acetone and DI water were used to avoid any sort of contamination. Compressed Air at 1 bar pressure was used for the deposition. The substrate and Nozzle height was maintained at 120 mm in all the depositions. The flow rate was maintained at 4 mL/min. Flow factor was taken at 1. The spray pyrolysis setup is shown in figure 1. The film prior to deposition was coated with 60-70 nm Copper using physical vapor deposition system. Presence of Copper film on the PI increased the adhesion of the ZnO. 50 ml of solution was sprayed for the preparation of each film. Subsequent spraying after shorter duration reduced the island formation of ZnO on the substrate and resulted in the thick uniform film. Polyimide films (50 μm), 'HN grade' was thoroughly cleaned in ultra sonicator for 5 minutes each in DI water, Acetone, Isopropyl Alcohol. The reaction in spray pyrolysis takes place as shown below.

$$Zn(CH_3COOH)_2 + H_2O + CH_3OH \longrightarrow Zn^{2+}(aq.) + OH^-(aq.) + CH_4\,(g) + 2CH_3COOH\,(aq) \quad (1)$$

$$Zn^{2+}(aq.) + OH^-(aq.) + CH_4\,(g) + 2CH_3COOH\,(aq) \longrightarrow Zn(OH)_2 \quad (2)$$

$$Zn(OH)_2 \longrightarrow ZnO(s) + H_2O(g) \quad (3)$$

The crystallinity and phase information were examined by powder XRD (Rigaku Smart Lab system) with CuKα radiation operating at 40 kV and 40 mA and with wave length λ = 1.5418 Å. The morphology and structures of the as-prepared ZnO nano rods and nanowalls were further studied by FESEM (Carl Zeiss Sigma series supra-55). The PL spectrometer (Dongwoo Optron DM 500i) having an excitation source consisting of a continuous wave He–Cd laser (excitation wavelength, 325 nm, PMT detector) was used to measure the PL emission from these samples at room temperature. Thermal Analysis was done using Mettler Toledo Thermal Analyzer for a range of 25-800 ºC with a step of 10 ºC/min. IV measurement was taken using Keithley Source measuring unit (SMU-2612).

3. Results and Discussion

3.1. Structural and morphological analysis

Figure 1 shows the XRD spectra of the ZnO films deposited at various temperatures. The diffraction peaks assigned to ZnO with hexagonal wurtzite structure. The film shows a polycrystalline nature and

peak positions are in agreement with the JCPDS (Card No. 36-1451). The peaks shows the crystalline phase of ZnO. Here we calculated the crystalline or grain size using well known Debye Scherrer's equation [8].

$$D = \frac{k\lambda}{\beta \cos\theta} \quad (4)$$

Where D = crystallite size, k = shape factor (0.9), λ= wavelength of X-Ray source, β = Full width Half maxima of the corresponding peak. The c-axis constant was found using the diffraction angle of the (002) peak and was used to estimate the stress in the ZnO film [9].

$$\sigma \sim -4.5\times10^{12}\left(\frac{c-c_o}{c_o}\right) \text{ dyn/cm}^2 \quad (5)$$

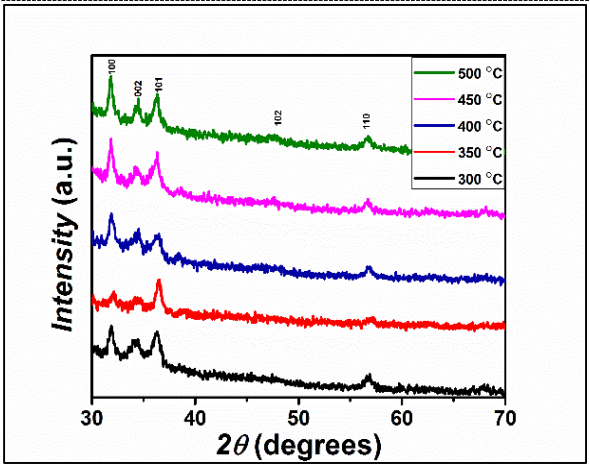

Figure 1. XRD analysis at different temperature.

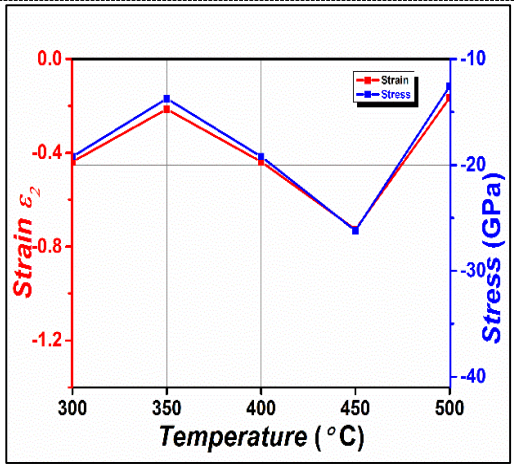

Figure 2. Stress-Strain analysis at different temperature.

Where c= calculated value and c_0= lattice constant of bulk which was taken as 5.2 Å. It was found that the film was having a compressive stress in the film. The change of stress with growth temperature have been resulted due to intrinsic effects (defects, impurities etc.) or extrinsic effects (lattice mismatch or thermal coefficient mismatch. It also account to the thermal coefficient mismatch of the substrate and the ZnO [10-12]. Compressive stress was observed in the film. The strain along c-axis (ε1) and strain in the plane (ε2) was also calculated using the following equations [13]

$$\varepsilon 1 = \frac{\text{dpowder} - \text{dfilm}}{\text{dpowder}} \times 100 \quad (6)$$

$$\varepsilon 2 = -\frac{\varepsilon 1}{\nu} \quad (7)$$

Where d_{powder} is the d spacing of the powder and taken as 0.2603 nm and d_{film} is the d spacing of the film calculated using Bragg's law. The values are tabulated in the table 1 and shown in figure 2.
Figure 2 shows as the stress increase the film strain in the plane increases. In all the above estimation of the stress and strain, the highest compressive stress is observed in film grown at 450 °C.

Table 1. Lattice and other parameter calculated using XRD graph

	c002(nm)	*D002(nm)*	*d002(nm)*	*Stress 002(GPa)*	Strain ξ1	strain ξ2
300	0.521481	7.6747	0.26074	-19.2	0.15765468	-0.4379297
350	0.521060	4.1138	0.26053	-13.7	0.07689746	-0.2136041
400	0.521481	7.6747	0.26074	-19.2	0.15765468	-0.4379297
450	0.522022	14.428	0.26101	-26.2	0.26166608	-0.7268502
500	0.52097	13.169	0.26048	-12.6	0.05947723	-0.1652146

As the temperature rises the stress is reduced due to High kinetic energy. In the film grown at 450 ºC the surface morphology is rough, with lots of visible cracks. High temperature favors rapid growth of crystallites due to oxidation of Zn atoms and optimum surface of diffusion of the species, whereas a low temperature results in the growth of disordered poorly crystallized structure. The development of a dense and uniform microstructures with good adhesion to the substrate is observed with increase of substrate temperature [14]. Moreover, around 350 ºC transition phase occurs where the reaction kinetics or growth rate is changed from surface diffusion controlled to mass transport controlled phenomenon [15-16]. Hence, the reaction kinetics is most favorable at 400 ºC.

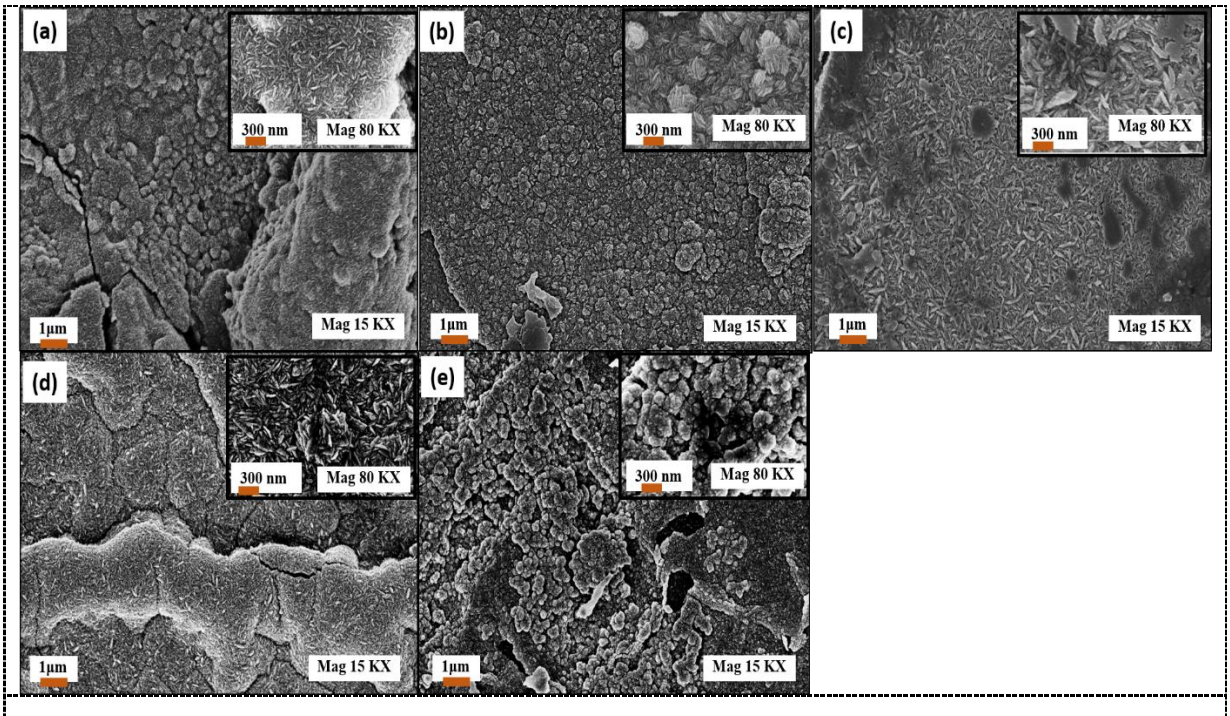

Figure 3. FE-SEM Micrograph of ZnO Deposited at (a) 300 ºC(b) 350 ºC(c) 400 ºC(d) 450 ºC and (e) 500 ºC

The Figure 3 shows the FE-SEM micrograph deposited at various temperatures. It is clear from the SEM Micrographs that the morphology is strongly dependent on temperature. At 300 °C the film shows uneven morphology in the film. It is observed that with increases in temperature the

morphology becomes uniform. At 400 ºC the smaller flakes increases in size. Further, upon increasing the temperature due to rapid cooling and heating at 450 and 500 °C surface morphology again distorts and cracks are visible. It accounts due to higher substrate temperature, the solution droplets have less time to distribute into homogeneous films due to faster solvent evaporation [17].

3.2. Photoluminescence Characterization

Figure 4 shows the room temperature Photoluminescence (PL) spectra of the ZnO deposited at various temperatures. The spectra shows the strong indication of Temperature inducing various defects in the film. The near band edge emission (NBE) was observed at 385 nm (λ_1), analogous to band gap of ZnO (3.31 eV) along with the Deep level Emission (DLE) [18].

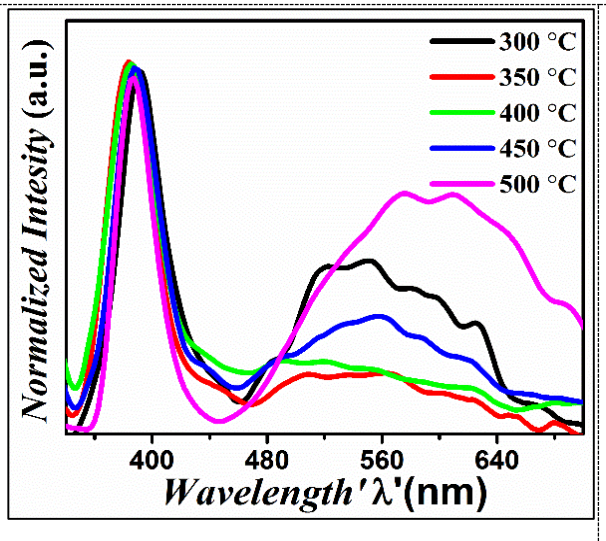

Figure 4. PL Spectra of ZnO deposited at various substrate temperatures

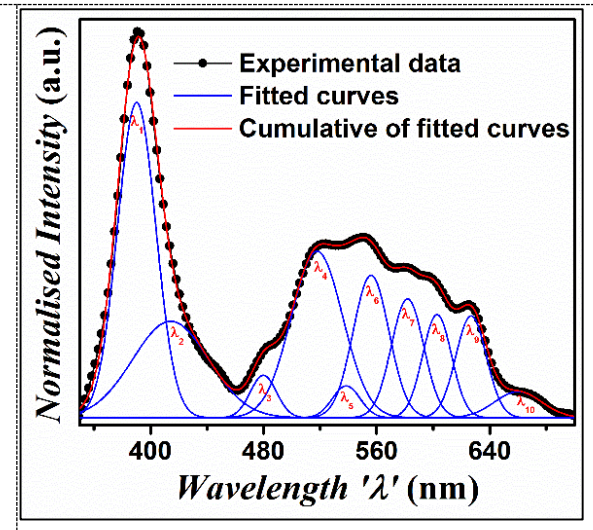

Figure 5. De-convoluted spectra showing well resolved peaks of PL at 300 °C.

The DLE intensity was found to decrease till 400 °C. Further increasing the temperature the DLE is again found to rise. The Figure 5 shows the PL spectra of Deposition at 300 °C which was de-convoluted into ten well resolved Gaussian peaks. The Broad emission peak positioned near 413 nm (λ_2) corresponding to 2.99 eV is supposed to be created from the swallow donor, Zn interstitial to valance band (VB). The green PL corresponding to the peak at 515(λ_4), 535 (λ_5) and 555(λ_6) nm had mostly been credited to the existence of oxygen vacancies [20–23]. Yellow photoluminescence peak were also detected at 582 nm (λ_7) corresponding to 2.13 eV is originated due to antisite oxygen defect state [19]. Two orange photoluminescence peaks at 605nm (λ_8) and 620 nm (λ_9) corresponding to 2.04 and 2.0 eV below the conduction band, these defects are created due to intricate of Oxygen Vacancy and Zinc interstitial cluster *i.e.* blend of two point imperfection [19]. The small wavelength peak at 660 nm (λ_{10}) corresponds to the second harmonic generation of the PL instrument which was used to excite the ZnO film at 325 nm. This corresponds to the improper filtration of signals in the instrument at excited frequency. This errors are usually small and can be attributed to instrument error.

3.3. Thermal Effects

The figure 6 shows the Thermogravimetric analysis of ZnO/Cu/PI films. The figure clearly shows that the appreciable thermal degradation of the Film starts around 555 °C. So the characterizing temperature on which the experiment were performed was way below the thermal degradation

temperature. This sudden decay in weight percentage accounts for the degradation of polyimide film. The graph follows the pattern as reported before. There is a slight variation in the weight at the initial stage near 200 °C which may corresponds to the release of trapped water vapors in the film [24]. It may also corresponds to the breaking of small amount of trapped zinc hydroxide into Zinc oxide and water vapors [4]. The graph also implies that it is safe to conduct experiments till 500 °C taking 50 °C as a factor of safety.

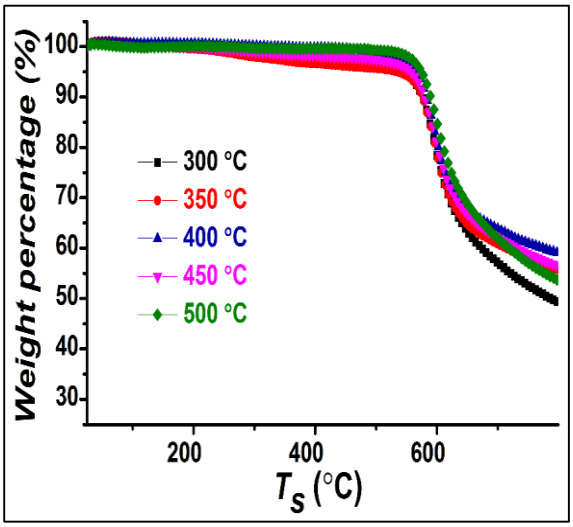

Figure 6. TGA analysis.

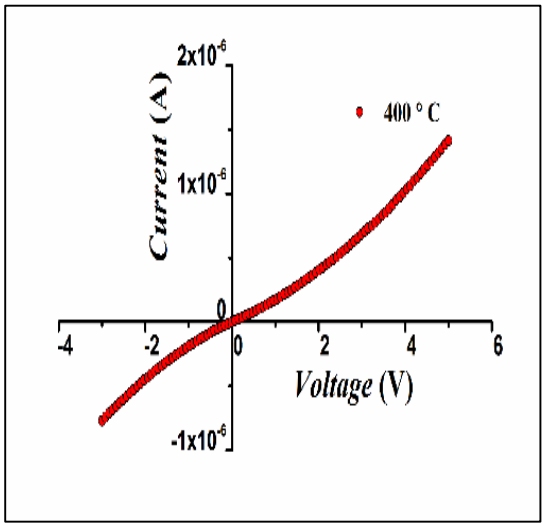

Figure 7. IV Characteristics of film deposited at 400 ºC.

3.4. IV Characteristics

The Figure 7 shows the IV characteristics of ZnO deposited at 400°C. The contacts for IV characterization was made using silver paste. A loop from -3 V to 5V was run and the current was measured. The IV characteristics appear to be proportional with respect to the bias. Consistent and precise results could only be obtained with a combination of Ohm's law for low voltages, as Ohm's law is usually valid for the low-voltage –intrinsic – regime of a low-conductivity material. Decent rectification behavior of the Schottky diodes was observed in the IV curve [25].

4. Conclusion

- Successfully deposited the ZnO over flexible substrate via a simple spray pyrolysis technique.
- Modified the conventional process and sprayed for shorter duration reduced island formation.
- Least lattice stress and strain in the film was observed at 450°C but surface morphology is uneven.
- Most uniform morphology and least defect was observed at 400°C.
- The IV characteristics of film grown at 400°C appear to be proportional with respect to the bias.

5. Acknowledgement

Authors are grateful to Sophisticated Instrument Centre, IIT Indore for providing characterization facilities. Author PR is grateful to the reviewers for the constructive help/comments received in the improvement of manuscript. Authors are also thankful to the Department of Science and Technology, India (DST) and Japanese Society for the Promotion of Science (JSPS) for promoting the Research.

References

[1] Z L Wang, Nanostructures of zinc oxide ISSN: 1369 7021, (2004).
[2] Tejendra Dixit, Ashish Kumar, I.A. Palani, Vipul Singh, Scripta Materialia 114, pp 84–87, (2016)
[3] Yi Qi, Noah T. Jafferis, Kenneth Lyons, Jr., Christine M. Lee, Habib Ahmad and Michael C. McAlpine Nano Lett., 10, pp 524-528 (2010)
[4] Tejendra Dixit, I. A. Palani, Vipul Singh, J Mater Sci: Mater Electron 26, pp 821–829, (2015)
[5] Manoj Kumar Gupta, Ju-Hyuck Lee, Keun Young Lee, and Sang-Woo Kim ACS Nano vol. 7, no. 10, pp 8932–8939, (2013)
[6] Woo-Suk Jung, Min-Gyu Kang, Hi Gyu Moon, Seung-Hyub Baek, Seok-Jin Yoon, Zhong-Lin Wang, Sang-Woo Kim & Chong-Yun Kang, Sci. Rep. 5, pp 9309, (2015).
[7] Shashank Priya, Daniel J. Inman (Eds.), Energy Harvesting Technologies, Springer Science & Business Media, 2008.
[8] B.D. Cullity, Elements of X-ray diffraction, 2nd edn. (Addison-Wesley, Reading, MA, 1979)
[9] R. Kumar, N. Khare, V. Kumar, G.L. Bhalla, Appl. Surf. Sci. 254, 6509 (2008)
[10] E.G. Bylander, J. Appl. Phys. 49, 1188 (1978)
[11] K. Vanheusden, C.H. Seager, W.L. Warren, D.R. Tallant, J.A.Voiget, Appl. Phys. Lett. 68, 403 (1996)
[12] M. Liu, A.H. Kitai, P. Mascher, J. Lumin. 54, 3 (1992)
[13] I. Ozen, M.A. Gulgun, Meric Ozcan, Key Eng. Mater. 262–268 (2004) 1225–1228.
[14] R. Mariappan, V. Ponnuswamy, R. Suresh, P. Suresh, A. Chandra Bose, M. Ragavendar, J Alloy Compd 582, pp 387–391, (2014)
[15] F. Paraguay D, W. Estrada L, D.R. Acosta N, E. Andrade, M. Miki-Yoshida, Thin Solid Films 350, pp 192-202, (1999).
[16] R. Ayouchi, F. Martin, D. Leinen, J.R. Ramos-Barrado, Journal of Crystal Growth 247, 497–504 (2003).
[17] Aneeqa Bashir, Paul H. Wobkenberg, Jeremy Smith, James M. Ball, George Adamopoulos, Donal D. C. Bradley, and Thomas D. Anthopoulos Adv. Mater. 21, pp 2226–2231, (2009).
[18] S. B. Zhang, S. H. Wei and A. Zunger, Phys. Rev. B: Condens. Matter Mater. Phys., 2001, 63, 075205.
[19] D. Behera and B.S. Acharya, J of lumin 128, 1577 (2008).
[20] J.P. Zhang, L.D. Zhang, L.Q. Zhu, Y. Zhang, M. Liu, X.J. Wang, J. Appl. Phys. 102, 114903 (2007)
[21] K. Vanheusden, C.H. Seager, W.L. Warren, D.R. Trallant, J. Caruso, J. Lumin. 75, 11 (1997)
[22] F.H. Leiter, H.R. Alves, A. Hofstaetter, D.M. Hofmann, B.K.Meyer, Phys. Stat. Sol. B R4, 226 (2001)
[23] K. Vanheusden, W.L. Warren, C.H. Seager, D.R. Trallant, J.A. Voigt, J. Appl. Phys. 79, 7983 (1996)
[24] Mansor Bin Ahmad, Yadollah Gharayebi, Mohd. Sapuan Salit , Mohd. Zobir Hussein, Saeideh Ebrahimiasl and Arash Dehzangi, Int. J. Mol. Sci. 13, pp 4860-4872 (2012)
[25] M. A. Lampert and P. Mark, Current Injection in Solids, Academic Press, New York, 1970.